Ann. For. Res. 69(1): 129-144, 2026
https://doi.org/10.15287/afr.2026.2684

ANNALS OF FOREST RESEARCH
www.afrjournal.org

Bee-inspired Radial Basis Function network to estimate tree aboveground wood volume in Brazilian Savanna

Natielle Gomes Cordeiro[1]✉, Kelly Marianne Guimarães Pereira[1,2], Eugênio Monteiro da Silva Júnior[3], Carlos Alberto Araújo Júnior[3], Renato Dourado Maia[3], Moisés Lima Dutra[4], Christian Dias Cabacinha[3]

Cordeiro N.G., Pereira K.M.G., Silva Júnior E.M., Araújo Júnior C.A., Maia R.D., Dutra M.L., Cabacinha C.D., 2026. Bee-inspired Radial Basis Function network to estimate tree aboveground wood volume in Brazilian Savanna. Ann. For. Res. 69(1): 129-144.

Abstract Forest variables such as aboveground wood volume are usually estimated by applying regression analysis. Nevertheless, in the past decades, new alternatives have been used, for example, artificial neural networks. In this sense, our study aimed to evaluate the efficiency of the Radial Basis Function (RBF) neural network in estimating aboveground wood volume for the Brazilian savanna using the cOptBees training algorithm. We fitted 18 allometric models and trained three Multilayer Perceptron (MLP) networks and two RBF networks using two different algorithms: k-means and cOptBees. We selected the MLP and RBF networks, as well as the allometric model with the best accuracy, for comparison. We verified the methods' accuracy by analysing the statistics of bias, root mean square error (RMSE), and Pearson's correlation coefficient. The lowest bias value was presented by the RBF network using the cOptBees algorithm (5.90×10^{-5}). The Näslund model showed the highest correlation (9.45×10^{-1}), as well as the lowest RMSE (2.07×10^{-3}). The aboveground wood volume estimates provided by the artificial neural networks showed similar results to those provided by classical regression models. Overall, we may infer that RBF networks trained using the cOptBees algorithm can be used to estimate aboveground wood volume in the Brazilian savanna, being as accurate as MLP or RBF networks trained with the k-means algorithm and allometric models. Finally, all methods showed similar aboveground wood volume estimates. However, neural networks offer advantages in optimizing field surveys because they require less sampling effort.

Keywords: cOptBees algorithm, artificial neural networks, volumetric models, Brazilian savanna.

Addresses: [1]Department of Forest Sciences, Federal University of Lavras, Lavras, MG, Brazil. | [2]Department of Ecology and Conservation, Federal University of Lavras, Lavras, MG, Brazil. | [3]Institute of Agricultural Sciences, Federal University of Minas Gerais, Montes Claros, MG, Brazil. | [4]Department of Information Science, Federal University of Santa Catarina, Florianópolis, SC, Brazil.

✉ **Corresponding Author:** Natielle Gomes Cordeiro (natiellegcordeiro@gmail.com).

Manuscript: received November 03, 2022; revised February 24, 2026; accepted March 10, 2026.

Introduction

Savanna ecosystems play an important role in providing a wide range of economic, social, and ecological benefits, including carbon sequestration, aboveground wood production, water and soil protection, and biodiversity conservation (Inkotte et al. 2022, Oliveira et al. 2024, Souza et al. 2024). Globally, savannas are found across Africa, India, Australia, Southeast Asia, South America and Central America (Grace et al. 2006, Pennington et al. 2018). In South America, the Brazilian savanna (known as Cerrado) stands out as the most biodiverse neotropical savanna, providing multiple ecosystem services (Bueno et al. 2016). The Brazilian savanna covers approximately 2 million km^2 and encompasses a mosaic of vegetation that includes grassland savanna (herbaceous vegetation represented mainly by grasses), densely wooded savanna (a stratum characterized by a predominance of arboreal trees), and woodland savanna (represented by spaced trees of 5-8 m in height) (Ribeiro & Walter 2008, Zimbres et al. 2021). In addition to the different vegetation types, the structural heterogeneity poses significant challenges to ecological assessment and stock estimates, such as aboveground wood production and carbon assimilation.

Trees at the Brazilian savanna commonly exhibit irregular forms, presenting crooked stems, tilted growth, and thick bark as adaptive responses to seasonal drought and fire events (Honda et al. 2014). The structural complexity, combined with the vast area and sampling effort required, results in high costs and time-consuming field-based biomass and volume measurements (Silveira et al. 2019). However, aboveground wood volume estimates in this vegetation type remain a crucial component of forest assessments, since wood production can serve as a reliable proxy for carbon stock (Naumov et al. 2018, Liu et al. 2019, Souza et al. 2024). Accurate estimation of the aboveground wood volume, beyond providing information on forest ecosystem carbon stock and sequestration, may also leads to insights into forest health, growth and yield, and management plans to address climate change (Binoti et al. 2013, Silva Júnior et al. 2018, Nordström et al. 2019).

Traditionally, aboveground wood volume is estimated by applying allometric models based on diameter at breast height (DBH) and total height (H) (Giri et al. 2019, Souza et al. 2024). However, in natural and heterogeneous ecosystems (with non-uniform vegetation) such as the Brazilian savanna, there is a great variability in tree shape and size, and therefore the relationship between DBH and H may not capture the full variability in tree architecture, resulting in lower predictive performance from the models (Sousa et al. 2023, Souza et al. 2024). To overcome this limitation, machine learning, especially the artificial neural networks (ANNs), has emerged as powerful tools in forest modelling (Miguel et al. 2015, Carrijo et al. 2020, Sousa et al. 2023, Oliveira et al. 2024). ANNs are capable of handling complex, nonlinear relationships and have been widely used in estimating forest variables, including aboveground wood volume, height-diameter relationship, total height, and biomass, among others (Ercanli 2020, Oliveira et al. 2021, Costa et al. 2022, Güner et al. 2022).

The most used ANN architectures for estimating forest variables are Multilayer Perceptron (MLP) and Radial Basis Function (RBF) (Cheshmberah et al. 2020, Günlü et al. 2021, Asl et al. 2024). While MLPs are known for their ability to solve complex problems with high degrees of non-linearity, RBF networks offer structural advantages, especially when the neurons in the hidden layer are defined by clustering algorithms (Haykin 1999, Silva Júnior et al. 2018, Zhang et al. 2018, Cheshmberah et al. 2020). Commonly, RBF networks are trained using the K-means algorithm, an unsupervised algorithm that requires the number of clusters to be predefined (Braga et al. 2014, Sousa Júnior et al. 2022, Soper 2023). In contrast, the cOptBees algorithm, a bio-inspired optimization technique based on bees' behavior, automatically determines the number of clusters and has demonstrated superior performance in pattern recognition and modeling tasks (Cruz et al. 2015, Cruz et al. 2016, Silva Júnior et al. 2018).

The cOptBees algorithm has been applied to estimate variables in planted forests (Silva Júnior et al. 2018), but until now its potential for modelling in natural, heterogeneous environments remains unexplored. The absence of studies applying cOptBees in natural ecosystems, such as the Brazilian savanna, does not necessarily indicate lack of potential, and indeed reflects the novelty of the method and the need for comparative evaluation. Considering the Brazilian savanna structural variability and the scarcity of high-resolution aboveground wood volume data, it is especially relevant to test whether algorithms capable of adaptive clustering can improve model performance over traditional methods. The greater variability of the data in natural forests represents a major challenge to regression algorithms (Bayat et al. 2021, Miranda et al. 2022). Meanwhile, the cOptBees algorithm shows great capacity in grouping similar data. Thus, this algorithm tends to cluster tree individuals exhibiting similar patterns, for example, belonging to the same species.

Therefore, the aim of our study is not only to apply the cOptBees algorithm in a new ecological context, but also to comparatively assess its performance against widely used modelling approaches. We evaluate four methods for estimating tree aboveground wood volume in the Brazilian savanna: (1) traditional allometric models; (2) MLP networks; (3) RBF networks trained with k-means; and (4) RBF networks trained with cOptBees. By analysing the strengths and limitations of each method in a complex and understudied biome, this study contributes to advancing forest modelling and supports improved forest assessment strategies in tropical savannas.

Material and methods

Study area

Our study covered a Brazilian savanna area (29.6 ha) in Minas Gerais state, southeast Brazil (Figure 1). The vegetation is classified as Woodland savanna ("Cerrado *sensu stricto*"), which is characterized by spaced trees with heights ranging from 5-8 m (Ribeiro & Walter 2008). The main woody tree species found in this vegetation type are *Byrsonima coccolobifolia*, *Curatella americana*, *Caryocar brasiliense*, and *Hancornia speciosa* (Ratter et al., 2003).

The region's climate is classified as Aw (according to the Köppen classification), a warm climate, with rainfall concentrated in the summer and a dry season in winter. The mean annual precipitation is 1086.4 mm and mean annual temperature is 23.1 °C. The soil classification is generally Cambisol (Alvares et al. 2013).

Data collection

A forest inventory was carried out during 2013 and 2014 at the forest remnant. For that, we systematically sampled a total of 25 plots of 20 × 20 m (400 m^2), covering a total area of one hectare. All arboreal trees with diameter at breast height (DBH) equal to or greater than 3 cm were measured. The total height of these trees was also recorded. Botanical material (flowers, leaves, and fruits from each tree) was collected and exsiccates were prepared for species identification (Lorenzi 1998, Silva-Júnior 2012). The taxonomy was standardized according to the Angiosperm Phylogeny Group IV system (APG 2016).

A total of 919 trees were identified during the forest inventory. However, we carried out the destructive sampling for aboveground wood volume estimates on only 586 trees. Some native species from the Brazilian savanna are legally protected due to their endangered status; therefore, these species were not included in the destructive sampling. Additionally, to ensure representation, we selected only species with at least eight individuals in the study area. We used the Huber method to measure the volume of branches and stems with a minimum diameter of 3 cm. This method consists of dividing each tree stem into straight segments and estimating the volume of each segment as the product of its cross-sectional area at the midpoint and its length (Equation 1) (Grosenbaugh 1948, Freese 1973). The diameter is measured at the midpoint of each segment, allowing accurate volume estimation even in irregularly shaped or tortuous stems.

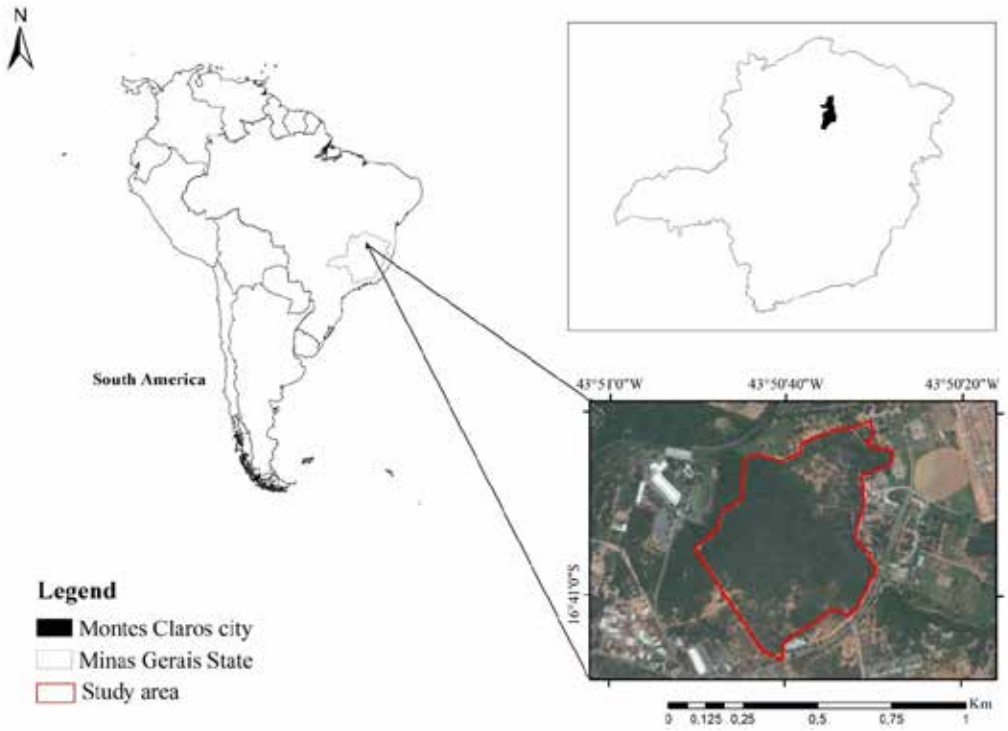

Figure 1 Study area of Cerrado *sensu stricto* located in Montes Claros, Minas Gerais, southeast Brazil.

$$V = g*L \quad (1)$$

where: V is aboveground wood volume of the *i-th* section (m^3); g is the *i-th* sectional area (meters); L is the section length of the stem or branch (meters).

For each tree, the stem was divided into n segments (depending on stem curvature), while respecting natural changes in direction along the trunk (Figure 2). We measured the total length of each segment and its diameter at the midpoint in the field using a measuring tape. The total tree volume was obtained by summing the segment volumes. This approach is particularly advantageous for species of the Brazilian savanna (Cerrado), which often exhibit stem tortuosity and irregular bole shapes. Unlike methods that assume a straight trunk (e.g., Smalian or Newton formulas), the Huber method allows adapting the measurement to each straight segment, reducing systematic errors in volume estimation.

We conducted a statistical analysis to assess data dispersion using boxplots. Through this analysis, we identified the presence of outliers and exclude them from the database. Overall, we used a total of 514 trees to fit the allometric models and to train the artificial neural network (MLP and RBF).

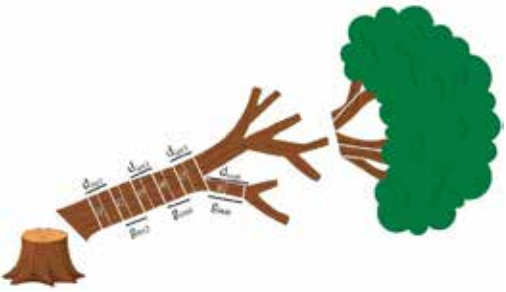

Figure 2 Schematic design of the Huber method used for destructive tree sampling. d is the measured diameter at the midpoint of each segment; l is the stem or branch length; g is the cross-sectional area.

Fitting of allometric models

We fitted 18 allometric models (see Table S1, supporting information) using regression analysis (Imaña-Encinas et al. 2009). The models were fitted using the *minpack.lm* package (Elzhov et al. 2016) in the R software (R Core Team 2017). We evaluated the fitted models based on the residual standard error values in m^3 (Syx) (Equation 2) and in percentage (Syx%) (Equation 3) (which were recalculated for the logarithmic models), significance of the parameters, adjusted coefficient of determination (R^2Adj.) (Equation 4), residual plots and Akaike Information Criterion (AIC) (Equation 5) (Thomas et al. 2006, Imaña-Encinas et al. 2009, Gujarati & Porter 2011). We ranked the models according to their statistical results to select the best one. Thus, scores were assigned for each statistic, in which the lowest scores were associated with the statistics with better performance. The best fitted model was selected for comparison with the artificial neural networks.

$$\mathrm{Syx} = \sqrt{\mathrm{MSE}} \tag{2}$$

$$\mathrm{Syx} = \frac{\mathrm{Syx}}{\bar{V}} * 100 \tag{3}$$

$$\mathrm{R^2\ Adj.} = 1 - \left(1 - \mathrm{R}^2\right) \frac{n-1}{n-K} \tag{4}$$

$$ln\mathrm{AIC} = \left(\frac{2K}{n}\right) + \ln\left(\frac{SSR}{n}\right) \tag{5}$$

where: MSE: Mean square error; $\bar{V}$ Mean aboveground wood volume; R^2 Adj.: Adjusted coefficient of determination; R^2: Coefficient of determination; K: equation number of coefficients; n: number of observations; SSR: Sum of squared residuals.

Artificial neural network training

We estimated the aboveground wood volume using different artificial neural network architectures. The input variables were diameter at breast height (DBH) and total height, while the output variable was aboveground wood volume. The tree diameter-height relationship is widely studied and described by mathematical models, and these metrics are commonly used for aboveground wood volume estimation, allowing inferences about forest productivity (Mugasha et al. 2013, Nascimento et al. 2020, Silveira et al. 2023). The data (diameter, height and aboveground wood volume) were normalized using the Min-Max normalization, which consists of a linear transformation of the data, homogenizing the magnitude of the variables (Gorgens et al. 2009, Yang et al. 2022). In this procedure, the minimum value of each variable is transformed to zero (0) and the maximum value to one (1) (Yang et al. 2022), while the remaining values are rescaled to the interval between 0 and 1 (Yang et al. 2022).

We used 70% of the data for training and 30% for validation. The dataset was randomly selected and used consistently across all networks. We fitted three MLP networks (using different architectures) and two RBF networks (trained using the k-means and cOptBees algorithms). MLP networks are widely used for estimating forest variables and generally provide robust predictive performance. This type of network consists of an input layer, one or more hidden layers, and an output layer (Carrijo et al. 2020). Thus, we tested different architectures to identify the best-performing configuration for aboveground wood volume estimation. Meanwhile, RBF networks typically include a single hidden layer. Advances in computational intelligence have highlighted the importance of testing alternative training algorithms for RBF networks, which justifies our evaluation of the k-means and cOptBees algorithms (Silva Júnior et al. 2018, Soper 2023). ANN training and validation were conducted using the MatLab® 2010 Neural Network Toolbox. The validation dataset was used to evaluate and compare the fitted models and networks.

Training and selection of the MLP network

We trained three different MLP network architectures. Each network had a different number of hidden layers and neurons per layer. Most practical problems can be solved

using a single hidden layer, whereas two or more layers may be required to approximate discontinuous functions (Braga et al. 2014). We trained all three architectures using the resilient backpropagation algorithm, which shows faster convergence and requires less memory for training than other algorithms (Saputra et al. 2017). We fixed the number of epochs at 500, as this value ensures network convergence and reduces the error training. The logistic sigmoid (*logsig*) activation function was used for the hidden layer, and the linear function (*purelin*) was used for the output layer.

The input layer of all MLP networks was designed with two neurons (DBH and height), and the output layer with one neuron (aboveground wood volume). The architectural differences among the networks were related to the hidden layer design (Silva Júnior et al. 2018). Specifically, MLP1 was designed with one hidden layer and a single neuron; MLP2 had one hidden layer and five neurons; MLP3 comprised two hidden layers, the first with five and the second with 2 neurons (Figure 3). The neurons were implemented using the sigmoidal and linear logistic functions for the hidden layers and the output layer, respectively.

The estimation accuracy of the artificial neural networks was evaluated using the mean square error (MSE) (Equation 6) and the mean absolute percentage error (MAPE) (Equation 7). The ANN with the highest accuracy was selected for comparison with the best-fitting allometric model and RBF networks.

$$MSE = \frac{1}{n}\sum_{i=1}^{n}\left(Y_i - \widehat{Y}_i\right)^2 \quad (6)$$

$$MAPE = \frac{100}{n}\sum_{i=1}^{n}\frac{\left|Y_i - \widehat{Y}_i\right|}{\left|Y_i\right|} \quad (7)$$

where: Y: Observed aboveground wood volume value; $\hat{Y}$: Estimated aboveground wood volume value; n: number of observations.

Training and selection of RBF networks

We trained two RBF networks using different clustering algorithms. We applied the k-means algorithm (RBF k-means) and the number of clusters was empirically set to five. We then implemented the cOptBees algorithm (RBF_BEE), with parameters defined as proposed in Table 1 (Silva Júnior et al. 2018). The activation function used for RBF training was based on the multivariate Gaussian function. The radius was defined using the standard deviation heuristic. Finally, we evaluated the accuracy of the RBF networks using MSE and MAPE.

Table 1 Parameters used in the cOptBees algorithm according to the methodology proposed by Silva Júnior et al. (2018). N is the size of the database.

Parameter	Value
Maximum number of clusters	N/2
Minimum number of bees	50
Maximum number of bees	100
Percentage of recruiters	90%
Recruitment rate	0.7
Recruited for each recruiter	5
Inhibition radius	0.002
Stop criterion	5 cycles without fitness evolution

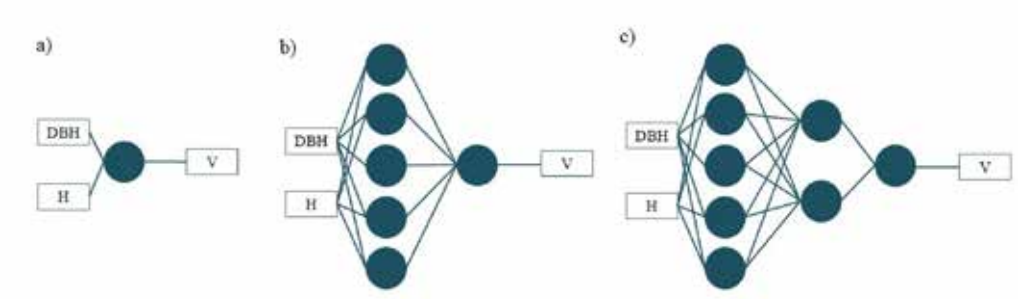

Figure 3 Architectural representation of the MLP1 (a), MLP2 (b) and MLP3 (c) networks, in which the input variables are DBH and H and output variable is V. DBH is diameter at breast height; H is total height; V is aboveground wood volume.

Comparison of the allometric model and ANNs

We compared the selected best-fitting allometric model, the best MLP network, and both RBF networks. We evaluated the models using root mean square error (RMSE) (Equation 8), Pearson's correlation coefficient (ry, ŷ) (Equation 9), bias (Equation 10) and percentage residual analysis based on histograms (Carrijo et al. 2020, Oliveira et al. 2024).

$$\mathrm{RMSE} = \sqrt{\frac{1}{n}\sum_{i=1}^{n}\left(Y_j - \widehat{Y}_j\right)^2} \quad (8)$$

$$r_{Y,\widehat{Y}} = \frac{\sum\left(Y\widehat{Y}\right) - \frac{(\sum Y)*\left(\sum \widehat{Y}\right)}{n}}{\sqrt{\left[\sum Y^2 - \frac{(\sum Y)^2}{n}\right]} * \sqrt{\left[\sum \widehat{Y}^2 - \frac{\left(\sum \widehat{Y}\right)^2}{n}\right]}} \quad (9)$$

$$\mathrm{Bias} = \frac{\sum e}{n} \quad (10)$$

where: Y: Observed aboveground wood volume value; Ŷ: Estimated aboveground wood volume value; e: Error (Observed aboveground wood volume value - Estimated aboveground wood volume value); n: Number of observations.

Results

Forest structure

A total of 514 tree individuals, belonging to 39 species, were included in our analysis. Among all species identified in the study area, 11 were identified only at the vernacular level. Overall, the most abundant species, in terms of number of individuals were *Albizia niopoides* (Spruce ex Benth.) Burkart (151), *Machaerium opacum* Vogel (74), and *Terminalia argentea* Mart. & Zucc. (33) (Table 2). Together, these three species accounted for more than 50% of the total measured trees used in our analysis, indicating a remnant dominated by few species. Tree diameter at breast height (DBH) ranged from 3.01 to 10.82 cm, and the total height varied between 1.94 and 13.50 m. Meanwhile, individual tree volume ranged from 0.0009 to 0.0296 m³ across species, reflecting substantial variability in tree form and biomass allocation. The structural heterogeneity among species and size classes highlights the importance of evaluating the performance of different volume estimation methods, as their accuracy may vary according to tree morphology and size distribution.

Allometric models

The fitted allometric models (see Table S2, supporting information) showed substantial variation in performance across the evaluated criteria.

The adjusted coefficient of determination (R^2adj) ranged from 0.8370 to 0.9556, indicating a generally strong fit for most equations. The highest R^2adj was found for the Näslund model (0.9556), followed by Dissescu–Meyer (0.9481), Rezende et al. (2006) modified (0.9461), and Meyer (0.8971), confirming their superior explanatory power for tree volume (see Table S3, supporting information). The Akaike Information Criterion (AIC) highlighted Meyer as the most parsimonious model (AIC = 4.56×10^{-6}), followed closely by the Näslund and Scolforo and Silva (1993) modified equations. These models also exhibited the lowest residual standard errors, with Meyer (Syx = 26.80%) and Näslund (Syx = 26.88%) outperforming the remaining equations. Residual–DBH scatterplots showed that the best-performing equations—those with higher R^2adj, lower Syx, and lower AIC—produced narrow residual bands, low dispersion, and no systematic trends across the DBH gradient (Figure 4). In contrast, lower-performing models displayed increased heteroscedasticity, a tendency toward over- and underestimation at small diameters, and occasional extreme deviations in the residuals.

The global ranking of the evaluated criteria revealed a clear separation between high- and low-performing equations (Figure 5, see also Table S4 in the supporting information). Näslund, Dissescu–Meyer, and Meyer consistently ranked among the top models, whereas the Spurr (arithmetic and logarithmic forms) and Takata models showed the weakest performance. These results provide a strong baseline for subsequent comparison with machine-learning approaches; therefore, we selected the Näslund model as the benchmark for comparison with artificial neural networks.

Table 2 Summary of the sampled tree species, showing the number of individuals (N) and the minimum and maximum values of diameter at breast height (DBH), total height, and measured aboveground wood volume.

Species		DBH		Height		Volume	
	N	Min	Max	Min	Max	Min	Max
Albizia niopoides (Spruce ex Benth.) Burkart	151	3.02	9.07	2.64	13.50	0.0017	0.0259
Amburana cearensis (Allemão) A.C.Sm.	3	3.21	5.98	3.24	6.27	0.0021	0.0100
Astronium fraxinifolium Schott	1	5.60	5.60	3.70	3.70	0.0059	0.0059
Byrsonima verbascifolia (L.) DC.	14	3.02	10.38	3.22	6.20	0.0009	0.0296
Copaifera langsdorffii Desf.	21	3.02	10.82	3.23	8.90	0.0014	0.0283
Cordiera sessilis (Vell.) Kuntze	12	3.18	7.48	2.95	6.65	0.0014	0.0152
Curatella americana L.	26	3.85	9.55	1.96	5.70	0.0030	0.0252
Dilodendron bipinnatum Radlk.	1	4.74	4.74	4.80	4.80	0.0057	0.0057
Eriotheca pubescens (Mart.) Schott & Endl.	1	9.23	9.23	6.10	6.10	0.0267	0.0267
Eugenia dysenterica DC.	3	4.14	7.00	3.80	5.26	0.0041	0.0159
Guapira noxia (Netto) Lundell	25	3.06	8.28	3.00	8.78	0.0012	0.0296
Indet 1	4	3.28	5.63	3.59	5.50	0.0017	0.0110
Indet 2	1	5.98	5.98	4.42	4.42	0.0085	0.0085
Indet 3	2	3.49	3.50	3.79	4.90	0.0017	0.0052
Indet 4	2	6.37	7.51	5.80	5.83	0.0090	0.0130
Indet 5	20	3.01	5.79	3.88	10.41	0.0012	0.0134
Indet 6	3	3.79	8.72	4.80	6.20	0.0028	0.0210
Indet 7	2	4.46	4.55	5.95	6.94	0.0060	0.0060
Indet 8	19	3.02	9.87	3.11	7.34	0.0020	0.0264
Indet 9	3	3.44	4.11	2.52	3.18	0.0027	0.0037
Indet 10	2	4.84	4.87	4.65	5.19	0.0035	0.0066
Indet 11	1	4.55	4.55	7.20	7.20	0.0078	0.0078
Leptolobium dasycarpum Vogel	13	3.02	7.96	2.63	5.07	0.0016	0.0158
Lithraea molleoides (Vell.) Engl.	1	8.37	8.37	5.00	5.00	0.0198	0.0198
Luehea paniculata Mart.	7	3.50	5.98	3.35	5.89	0.0020	0.0072
Machaerium opacum Vogel	74	3.34	10.50	1.94	6.30	0.0022	0.0293
Magonia pubescens A.St.-Hil.	13	3.02	9.14	3.30	6.06	0.0014	0.0284
Maprounea guianensis Aubl.	2	4.30	4.87	3.42	3.48	0.0048	0.0057
Plathymenia reticulata Benth.	3	4.90	9.96	4.82	5.42	0.0058	0.0290
Psidium firmum O.Berg	3	3.50	5.57	3.71	6.60	0.0023	0.0084
Psidium sp.	2	3.63	5.47	3.81	5.56	0.0019	0.0077
Qualea grandiflora Mart.	1	3.60	3.60	4.60	4.60	0.0028	0.0028
Qualea parviflora Mart.	1	9.26	9.26	6.45	6.45	0.0225	0.0225
Roupala montana Aubl.	8	3.02	8.21	3.75	5.90	0.0015	0.0213
Tachigali aurea Tul.	10	3.60	7.96	2.95	5.21	0.0026	0.0166
Terminalia argentea Mart. & Zucc.	33	3.34	9.33	3.30	13.49	0.0018	0.0289
Tocoyena formosa (Cham. & Schltdl.) K.Schum.	19	3.34	6.40	2.70	6.50	0.0015	0.0117
Xylopia aromatica (Lam.) Mart.	5	3.06	4.06	5.55	10.50	0.0013	0.0081
Xylopia frutescens Aubl.	2	3.88	5.89	4.79	5.30	0.0035	0.0165

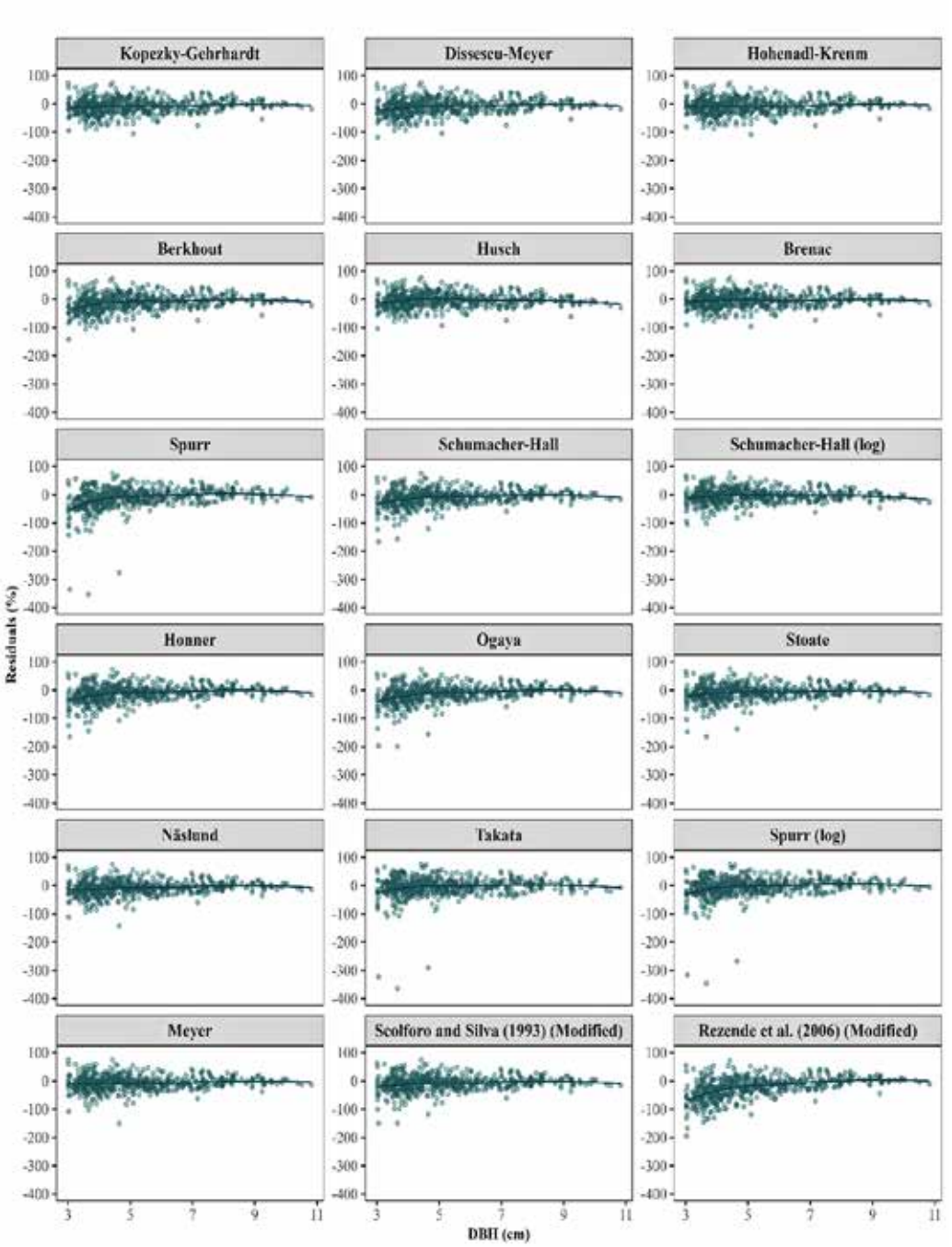

Figure 4 Residual distribution (%) as a function of DBH for the 18 models fitted to the Cerrado *sensu stricto* fragment in Montes Claros, Minas Gerais, southeast Brazil.

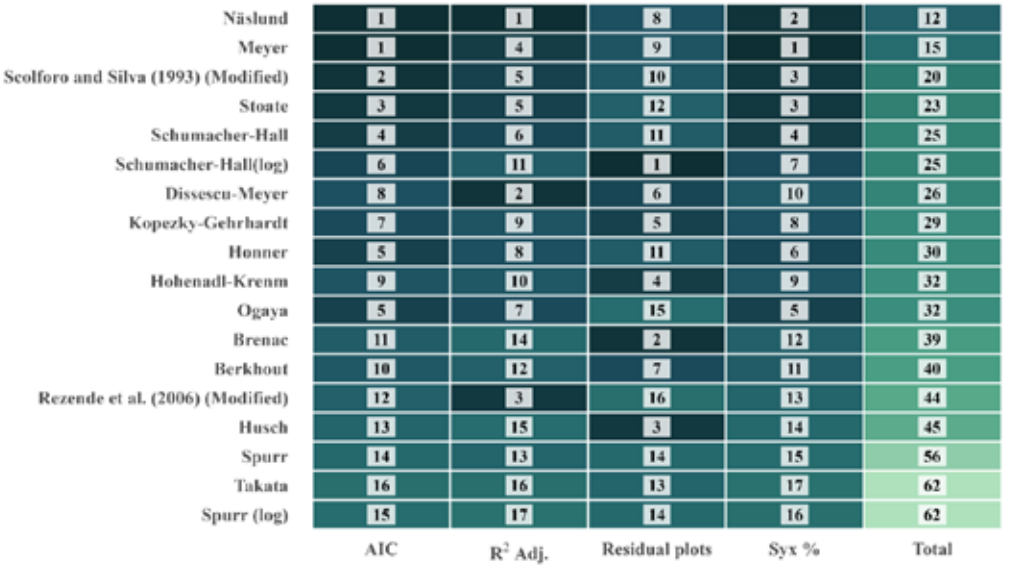

Figure 5 Global ranking of each allometric model according to the evaluated criteria.

Artificial neural networks

The three multilayer perceptron architectures exhibited similar error magnitudes, indicating that increasing network complexity did not translate into meaningful gains in predictive accuracy (Table 3). MLP3 showed the highest MSE and MAPE values, suggesting reduced generalization capacity, possibly associated with overfitting. Although MLP2 achieved the lowest MAPE (18.02%), MLP1 combined the lowest MSE with the simplest architecture, providing the most efficient balance between accuracy and parsimony. For this reason, we selected MLP1 as the representative MLP model for subsequent comparisons.

The two radial basis function networks showed nearly identical MSE values (1.7 x 10^{-3} for RBF k-means and 1.8 x 10^{-3} for RBF_BEE), indicating stable performance regardless of the training algorithm (Table 3). The slightly higher MAPE observed for RBF_BEE suggests a marginally less consistent error distribution across the dataset, although the difference was not substantial. Given that the two RBF models rely on distinct optimization procedures, we retained both to allow a broader assessment of how algorithmic design influences predictive performance.

Table 3 Mean square error and mean absolute percentage error for MLP and RBF networks trained on data from a Cerrado *sensu stricto* fragment in Montes Claros, Minas Gerais, southeast Brazil.

Network	MSE	MAPE
MLP1	1.7 x 10^{-3}	18.2275
MLP2	1.8 x 10^{-3}	18.0232
MLP3	2.1 x 10^{-3}	21.7332
RBF k-means	1.7 x 10^{-3}	17.7735
RBF_BEE	1.8 x 10^{-3}	18.7116

Comparison of the allometric model and the ANNs

The Näslund model and the three selected networks (MLP1, RBF_BEE and RBF k-means) showed minor differences in bias magnitude, error dispersion, and correlation strength (Table 4). The lowest bias was found to the RBF_BEE (5.90 x 10^{-5}), followed by MLP1 (1.33 x 10^{-4}), Näslund (1.40 x 10^{-4}) model and, RBF k-means (1.76 x 10^{-4}). RMSE values were nearly identical across all methods (2.06–2.12 x 10^{-3}), reinforcing that model choice had little influence on overall predictive precision.

The selected allometric model and neural networks revealed a consistent residual structure

among the methods (Figure 6). Most residuals were concentrated within the ±10% range across all methods, indicating stable error behaviour across architectures and the allometric model. Differences occurred mainly in the tails: RBF k-means showed a slightly narrower spread, whereas Näslund and MLP1 exhibited similar dispersion patterns. These results suggest that none of the methods introduced substantial systematic deviations, and that residual behaviour was robust to changes in modelling strategy.

Table 4 Accuracy analysis of the MLP and RBF networks and the Näslund model for estimating aboveground wood volume using data from a Cerrado *sensu stricto* fragment in Montes Claros, Minas Gerais, southeast Brazil. RMSE: Root mean square error; r: Pearson's correlation coefficient.

Methods	Bias	RMSE	r
Näslund Model	1.40×10^{-4}	2.06×10^{-3}	0.944703
MLP1	1.33×10^{-4}	2.07×10^{-3}	0.944623
RBF_BEE	5.90×10^{-5}	2.12×10^{-3}	0.941898
RBF k-means	1.76×10^{-4}	2.09×10^{-3}	0.943645

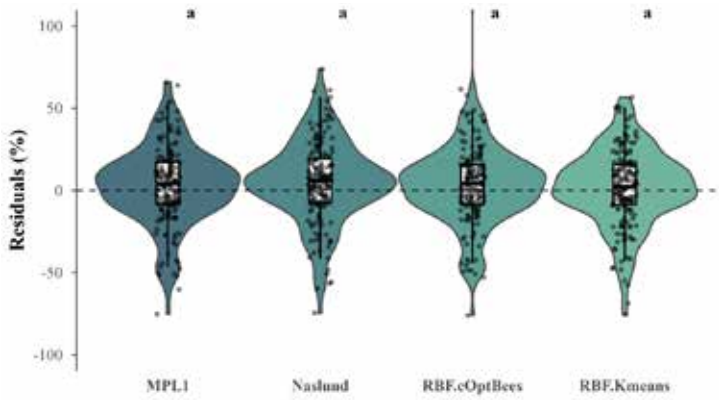

Figure 6 Residual plots for the Näslund model, MLP1, RBF K-means, and RBF_BEE, best fitted to the data from a Cerrado *sensu stricto* fragment in Montes Claros, Minas Gerais, southeast Brazil.

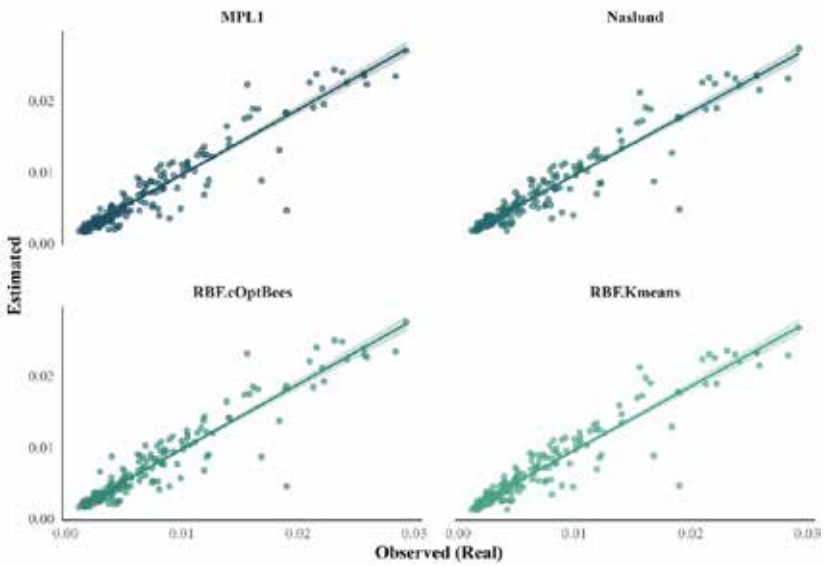

Figure 7 Observed versus predicted individual-tree aboveground wood volume for the four modelling methods (MLP-L1, Näslund, RBF-OptBees, and RBF-Kmeans). The 1:1 line indicates the ideal agreement between measured and estimated values.

The observed-versus-estimated aboveground wood volume values (Figure 7) confirmed the convergence in predictive performance between the allometric model and the neural networks. All methods produced strong linear correlations ($r \approx 0.94$) with minimal deviation around the 1:1 line, indicating that the neural networks - regardless of architecture or training algorithm - performed similarly to the traditional Näslund model in capturing the underlying volume patterns in the dataset.

Discussion

We assessed whether artificial neural networks could improve and optimize aboveground wood volume estimates. Overall, we found that choosing among MLP1, RBF_BEE, RBF k-means, or an allometric model such as the Näslund model resulted in only marginal differences in predictive performance. Predictive behaviour was largely invariant across methods, suggesting that model selection may prioritize interpretability, computational efficiency, or operational simplicity rather than gains in accuracy.

Forest structure

Overall, most tree individuals in the forest remnant are concentrated in the 4-8 cm diameter class (315 individuals), followed by individuals with diameter lower than 4 cm (155 individuals) and trees with diameter greater than 8 cm (44 individuals). Usually, greater biomass stocks in areas of Cerrado *sensu stricto* are typically associated with small-sized trees, as they represent the majority of individuals in this vegetation type (Rezende et al., 2006). This structural pattern and distribution into the remnant are a real reflection of the vegetation type that shows great variability. In other words, the remnant presents a range of diameter–height combinations which may directly impact the models fitting (Rezende et al. 2006).

The allometric relationship between DBH, height, and aboveground wood volume tends to follow a stable and predictable pattern when intermediate sizes dominate the dataset. Thus, this structure can make estimation task less sensitive to the choice of modelling method. The low number of trees in the largest diameter class may constrain the capacity of neural networks to learn nonlinear patterns at the extremes, where aboveground wood volume increases more rapidly and differences among models typically become more evident (Sousa et al. 2023). In this scenario, both the allometric model and the neural networks learn primarily from the densest region of the predictor space, which helps explain the convergence in performance observed across methods.

Allometric models and artificial neural networks

Classical regression models remain among the most widely applied methods for estimating forest variables, such as the aboveground wood volume in natural forests (Reis et al. 2020). These methods often achieve high accuracy because they rely on field-measured data as predictors (Silveira et al. 2019). Several studies have reported that the Schumacher-Hall model typically produces accurate estimates and is therefore broadly used to predict aboveground wood volume in natural forests (Gorgens et al. 2009, Binoti et al. 2014, Sousa et al. 2023). However, alternative regression models have also shown strong performance in Brazilian savanna ecosystems (Imaña-Encinas et al. 2009, Bueno et al. 2020) due to the vegetation idiosyncrasies (Zimbres et al. 2021, Sousa et al. 2023). In our study, the Näslund model yielded the best performance, corroborating its suitability for aboveground wood volume estimation in Brazilian savanna areas (Xavier et al. 2017).

Performing forest inventories is an essential tool for quantifying and characterizing natural resources. Nevertheless, this activity requires highly qualified labor and considerable field effort, which results in high operational costs (Silveira et al. 2019, Reis et al. 2020). Over the years, new approaches have been developed to optimize forest inventories and dataset processing (Reis et al. 2020). For example, artificial neural networks have shown great accuracy in estimating individual tree height, aboveground

wood volume, and forest structure classification (Binoti et al. 2013, 2014, Know et al. 2017). We also found good results using artificial neural networks in estimating aboveground wood volume, confirming the robustness of this approach. Indeed, previous studies on forest variables have demonstrated that network architectures with a single neuron in the hidden layer can provide reliable predictions (Binoti et al. 2014). This finding may help explain the performance of MLP1 in our study.

The architecture of artificial neural networks is mainly defined by the number of neurons and hidden layers. RBF networks, whose architecture may be defined using a clustering algorithm, tend to be simpler and require fewer parameters than an MLP network (Cruz et al. 2016, Silva Júnior et al. 2018). In addition, the output of a neural network neuron is generated by an activation function, which considers the interaction between the input values x and the weight vectors w (Binoti et al. 2014, Karlik & Olgak 2011).

Within this framework, RBF networks rely on radial basis functions, such as the Gaussian function, to perform nonlinear mapping (Braga et al. 2014). The use of a multivariate function is justified by characteristics such as input data dimensionality and the grouping process of each function. In the RBF_BEE network, grouping is determined by variations in the radius value (Cerqueira et al. 2001, Leon-Delgado et al. 2018). Accordingly, the efficiency of the artificial neural network architecture depends on the training algorithm's ability to determine an exact or approximate number of groups. For example, the cOptBees algorithm is characterized by its capacity to automatically form groups. Consequently, RBF network training using the cOptBees algorithm shows as good results as the MPL networks (Silva Júnior et al. 2018).

From a broader methodological perspective, the accuracy gains in estimations by artificial neural networks compared to classical regression models have been confirmed by several studies (Binoti et al. 2015, Miguel et al. 2015, Nunes & Görgens 2016). The RMSE values found in our study for the regression model and neural networks were quite small. Despite the strong performance of artificial neural networks, none outperformed the other methods. This same pattern was observed by Silva Júnior et al. (2018) when estimating eucalyptus aboveground wood volume using RBF neural networks. The authors also found better results using the cOptBees algorithm compared to random initialization and k-means algorithms. The application of the cOptBees clustering algorithm provided similar estimates for RBF networks in relation to MLP networks and allometric models.

Our findings indicate that the allometric model and both artificial neural networks (MLP and RBF) showed great accuracy and can be used for predicting forest variables. We observed that the predictive accuracy obtained by the four methods was similar. Therefore, we performed a hypothesis test to evaluate this similarity. The Wilcoxon test allowed us to infer that the distribution of errors for all evaluated methods is statistically equivalent, since the null hypothesis was not rejected in any case. Several studies on estimating forest variables describe more accurate results by using MLP networks, thus defining this network type as superior (Binoti et al. 2012, 2015, Reis et al. 2019). Nevertheless, our findings indicate the RBF network as a viable alternative, since it has great capacity to adapt to different datasets (Silva Júnior et al. 2018).

Conclusion

The aboveground wood volume estimates provided by artificial neural networks were similar to those provided by classical regression models. The use of artificial neural networks represents an important advantage, as their application may optimize field studies by reducing the sampling effort required to model development. The RBF trained using the cOptBees algorithm may be applied to estimate the aboveground wood volume of native species, showing to be as accurate as using MLP networks and allometric models. Further studies considering the RBF network, as well as the cOptBees algorithm, should be carried out in other areas with different vegetation types.

Acknowledgments

We express our gratitude to the Institute of Agrarian Sciences, Federal University of Minas Gerais (UFMG) and Federal University of Lavras (UFLA) for the support and infrastructure to the study development. This study was partly supported by the Coordenação de Aperfeiçoamento de Pessoal de Nível Superior - Brasil (CAPES) - Finance Code 001. In addition, the authors thank to the Fundação de Amparo à Pesquisa do Estado de Minas Gerais (FAPEMIG). We also thank CNPq (National Council for Scientific and Technological Development).

Supporting Information

Table S1 Aboveground wood volume models fitted to the Cerrado *sensu stricto* fragment data in Montes Claros, Minas Gerais, southeast Brazil.

Table S2 Coefficients of the aboveground wood volume models fitted to the Cerrado *sensu stricto* fragment data in Montes Claros, Minas Gerais, southeast Brazil.

Table S3 Statistical parameters analysis of the aboveground wood volume models fitted to the Cerrado *sensu stricto* fragment in Montes Claros, Minas Gerais, southeast Brazil.

Table S4 Statistics ranking used to assess the aboveground wood volume models fitted to the Cerrado *sensu stricto* fragment data in Montes Claros, Minas Gerais, southeast Brazil.

Author contribution statement

NGC: conceptualization, methodology, data curation, investigation, visualization, and writing – original draft preparation, as well as writing – review & editing; KMGP: conceptualization, methodology, and writing – review & editing; EMSJ: methodology, formal analysis, and data curation; CAAJ, RDM, and MLD: supervision; CDC: the resources, conceptualization, supervision, and project administration.

Conflict of interest

The authors declare no financial or personal interests could influence the work presented in this paper.

References

Alvares C.A., Stape J.L., Sentelhas P.C., Gonçalves J.L. de M., Sparovek G., 2013. Köppen's climate classification map for Brazil. Meteorologische Zeitschrift 22: 711–728. https://doi.org/10.1127/0941-2948/2013/0507.

Asl S.L., Navroodi I.H., Kalteh A.M., 2024. Sensitivity analysis and performance evaluation of neural networks for predicting forest stand volume – A case study: District 2, Kacha, Guilan province, Iran. Journal of Forest Science 70: 209-222. https://doi.org/10.17221/111/2023-JFS.

APG, 2016. An update of the Angiosperm Phylogeny Group classification for the orders and families of flowering plants: APG IV. Botanical Journal of the Linnean Society 181: 1-20. https://doi.org/10.1111/boj.12385.

Bayat M., Bettinger P., Hassani M., Heidari S., 2021. Ten-year estimation of Oriental beech (Fagus orientalis Lipsky) volume increment in natural forests: a comparison of an artificial neural networks model, multiple linear regression and actual increment. Forestry 94: 598-609. https://doi.org/10.1093/forestry/cpab001.

Binoti D.H.B., Binoti M.L.M. da S., Leite H.G., 2014. Configuração de redes neurais artificiais para estimação do volume de árvores. Revista Ciência da Madeira 5: 58-67. https://doi.org/10.1590/S0100-67622014000200008.

Binoti D.H.B., Binoti M.L.M. da S., Leite H.G., Silva A., Santos A.C. de A., 2012. Modelagem da distribuição diamétrica em povoamentos de Eucalipto submetidos a desbate utilizando autômatos celulares. Revista Árvore 36: 931–939. https://doi.org/10.1590/S0100-67622012000500015.

Binoti M.L.M. da S., Binoti D.H.B., Leite H.G., 2013. Aplicação de redes neurais artificiais para estimação da altura de povoamentos equiâneos de Eucalipto. Revista Árvore 37: 639–645. https://doi.org/10.1590/S0100-67622013000400007.

Binoti M.L.M. da S., Leite H.G., Binoti D.H.B., Gleriani J.M., 2015. Prognose em nível de povoamento de clones de Eucalipto empregando Redes Neurais Artificiais. Cerne 21: 97–105. https://doi.org/10.1590/01047760201521011153.

Braga A. de P., Carvalho A.P. de L.F. de, Ludermir T.B., 2014. Redes neurais artificiais - Teoria e aplicações. LTC – Livros Técnicos e Científicos Editora Ltda, Rio de Janeiro, 226 p.

Bueno L.P., Medanha J.T.R., Rodovalho R.S., Castro V.G.S. de, 2020. Modelagem volumétrica para frutíferas do Cerrado. Revista Mirante 13: 39-54.

Bueno M.L., Pennington R.T., Dexter K.G., Kamino L.H.Y., Pontara V., Neves D.M., Ratter J.A., Oliveira Filho A.T. de, 2016. Effects of Quaternary climatic fluctuations on the distribution of Neotropical savanna tree species. Ecography 39: 001–012. https://doi.org/10.1111/ecog.01860.

Carrijo J.V.N., Miguel E.P., Vale A.T.do, Matricardi E.A.T., Monteiro T.C., Rezende A.V., Inkotte J., 2020. Artificial intelligence associated with satellite data in predicting energy potential in the Brazilian savanna woodland area. iForest – Biogeosciences and Forestry 13: 48-55. https://doi.org/10.3832/ifor3209-012.

Cerqueira E.O. de, Andrade J.C. de, Poppi R.J., Mello C., 2001. Redes Neurais e suas aplicações em calibração multivariada. Química Nova 24: 864–873. https://doi.org/10.1590/S0100-40422001000600025.

Cheshmberah F., Fathizad H., Parad G.A., Shojaeifar S., 2020. Comparison of RBF and MLP neural network performance and regression analysis to estimate carbon

sequestration. International Journal of Environmental Science and Technology 17: 3891–3900. https://doi.org/10.1007/s13762-020-02696-y.

Costa E.A., Hess A.F., Finger C.A.G., Schons C.T., Klein D.R., Barbosa L.O., Borsoi G.A., Liesenberg V., Bispo P.C., 2022. Enhancing Height Predictions of Brazilian Pine for Mixed, Uneven-Aged Forests Using Artificial Neural Networks. Forests 13: 1284. https://doi.org/10.3390/f13081284

Cruz D.P.F., Maia R.D., Castro L.N. de, 2015. On the Sensitivity of a Bee-Inspired Algorithm to Its Internal Parameters. International Journal of Computer Information Systems and Industrial Management Applications 7: 84–93.

Cruz D.P.F., Maia R.D, Silva L.A. da, Castro L.N. de, 2016. Neurocomputing BeeRBF: A bee-inspired data clustering approach to design RBF neural network classifiers. Neurocomputing 172: 427–437. https://doi.org/10.1016/j.neucom.2015.03.106.

Elzhov T.V., Mullen K.M., Spiess A.-N., Bolker B., 2016. R Interface to the Levenberg-Marquardt Nonlinear Least-Squares Algorithm Found in MINPACK, Plus Support for Bounds. [online 16 April 2020] URL: https://cran.rproject.org/web/packages/minpack.lm/ minpack.lm.pdf.

Ercanli I., 2020. Artificial intelligence with deep learning algorithms to model relationships between total tree height and diameter at breast height. Forest systems 29: e013. https://doi.org/10.5424/fs/2020292-16393.

Freese F., 1973. A collection of log rules. Gen. Tech. Rep. FPL-1. U.S. Department of Agriculture, Forest Service, Forest Products Laboratory, Madison, 65 p.

Giri K., Jayaraj R.S.C., Pandey R., Nainamalai R., Ashutosh S., 2019. Regression equations for estimating tree volume and biomass of important timber species in Meghalaya, India. Current Science 116: 75–81. https://doi.org/10.18520/cs/v116/i1/75-81.

Gorgens E.B., Leite H.G., Santos H. do N., Gleriani J.M., 2009. Estimação do volume de árvores utilizando redes neurais artificiais. Revista Árvore 33: 1141–1147. https://doi.org/10.1590/S0100-67622009000600016.

Grace J., José J.S., Meir P., Miranda H.S., Montes R.A., 2006. Productivity and carbon fluxes of tropical savannas. Journal of Biogeography 33: 387-400. https://doi.org/10.1111/j.1365-2699.2005.01448.x.

Grosenbaugh L.R., 1948. Improved cubic volume computation. Journal of Forestry, 46: 299-301.

Gujarati D.N., Porter D.C., 2011. Econometria Básica. AMGH Editora Ltda, Porto Alegre, 924 p.

Güner S.T., Diamantopoulou M.J., Poudel K.P., Çömez A., Özçelik R., 2022. Employing artificial neural network for effective biomass prediction: An alternative approach. Computers and Eletronics in Agriculture 192: 106596. https://doi.org/10.1016/j.compag.2021.106596.

Günlü A., Ercanli I., Senyurt M., Keleş S., 2021. Estimation of some stand parameters from textural features from WorldView-2 satellite image using the artificial neural network and multiple regression methods: a case study from Turkey. Geocarto International 36: 918-935. https://doi.org/10.1080/10106049.2019.1629644.

Haykin S.S., 1999. Neural Networks: A Comprehensive Foundation. Prentice Hall, Hoboken, 842 p.

Honda E.A., Mendonça A.H., Durigan G., 2014. Factors affecting the stemflow of trees in the Brazilian Cerrado. Ecohydrology 8:1351-1362. https://doi.org/10.1002/eco.1587.

Imaña-Encinas J., Santana O.A., Paula J.E. de, Imaña C.R., 2009. Equações de volume de madeira para o Cerrado de Planaltina de Goiás. Floresta 39: 107–116. https://doi.org/10.5380/rf.v39i1.13731.

Inkotte J., Bomfim B., Silva S.C., Valadão M.B.X., Rosa M.G., Viana R.B., Rios P.D., Gatto A., Pereira R.S., 2022. Applied Soil Ecology 169: 104209. https://doi.org/10.1016/j.apsoil.2021.104209.

Karlik B., Olgac A.V., 2011. Performance Analysis of Various Activation Functions in Generalized MLP Architectures of Neural Networks. International Journal of Artificial Intelligence and Expert Systems 1: 111–122.

Know S.-K., Jung H.-S., Baek W.-K., Kim D., 2017. Classification of Forest Vertical Structure in South Korea from Aerial Orthophoto and Lidar Data Using an Artificial Neural Network. Applied Sciences 7: 1046. https://doi.org/10.3390/app7101046.

Leon-Delgado H. de, Praga-Alejo R.J., Gonzalez-Gonzalez D.S., Cantú-Sifuentes M., 2018. Multivariate Statistical Inference in a Radial Basis Function Neural Network. Expert Systems with Applications 93: 313–321. https://doi.org/10.1016/j.eswa.2017.10.024.

Liu J., Wang X., Wang T., 2019. Classification of tree species and stock volume estimation in ground forest images using Deep Learning. Computers and Electronics in Agriculture 166: 105012. https://doi.org/10.1016/j.compag.2019.105012.

Lorenzi H., 1998. Árvores brasileiras: manual de identificação e cultivo de plantas arbóreas nativas do Brasil. Instituto Plantarum de Estudos da Flora Ltda, Nova Odessa, 384 p.

Miguel E.P., Rezende A.V., Leal F.A., Matricardi E.A.T., Vale A.T. do, Pereira R.S., 2015. Redes neurais artificiais para a modelagem do volume de madeira e biomassa do cerradão com dados de satélite. Pesquisa Agropecuária Brasileira 50: 829–839. https://doi.org/10.1590/S0100-204X2015000900012.

Miranda E.N., Barbosa B.H.G., Silva S.H.G., Monti C.A.U., Tng D.Y.P., Gomide L.R., 2022. Variable selection for estimating individual tree height using genetic algorithm and random forest. Forest Ecology and Management 504: 119828. https://doi.org/10.1016/j.foreco.2021.119828.

Mugasha W.A., Eid T., Bollandsås O.M., Malimbwi R.E., ChamshamaS.A.O., Zahabu E., Katani J.Z., 2013. Allometric models for prediction of above- and belowground biomass of trees in the miombo woodlands of Tanzania. Forest Ecology and Management 310: 87-101. https://doi.org/10.1016/j.foreco.2013.08.003.

Nascimento R.G.M., Vanclay J.K., Figueiredo Filho A., Machado S. do A., Ruschel A.R., Hiramatsu N.A., Freitas L.J.M. de, 2020. The tree height estimated by non-power models on volumetric models provides reliable predictions of wood volume: The Amazon species height modelling issue. Trees, Forests and People 2: 100028. https://doi.org/10.1016/j.tfp.2020.100028.

Naumov V., Manton M., Elbakidze M., Rendenieks Z., Priednieks J., Uhlianets S., Yamelynets T., Zhivotov A., Angelstam P., 2018. How to reconcile wood production and biodiversity conservation? The Pan-European boreal forest history gradient as an “experiment”. Journal of Environmental Management 218: 1-13. https://doi.org/10.1016/j.jenvman.2018.03.095.

Nordström E.-V., Nieuwenhuis M., Başkent E.Z., Biber P., Black K., Borges J.G., Bugalho M.N., Corradini G., Corrigan E., Eriksson L.O., Felton A., Forsell N., Hengeveld G., Hoogstra-Klein M., Korosuo A., Lindbladh M., Lodin I., Lundholm A., Marto M., Masiero M., Mozgeris G., Pettenella D., Poschenrieder W., Sedmak R., Tucek J.,

Zoccatelli D., 2019. Forest decision support systems for the analysis of ecosystem services provisioning at the landscape scale under global climate and market change scenarios. European Journal of Forest Research 138:561–581. https://doi.org/10.1007/s10342-019-01189-z.

Nunes M.H., Görgens E.B., 2016. Artificial Intelligence Procedures for Tree Taper Estimation within a Complex Vegetation Mosaic in Brazil. Plos One 11: e0154738. https://doi.org/10.1371/journal.pone.0154738.

Oliveira D.V. de, Rode R., Oliveira Neto R.R. de, Gama J.R.V., Leite H.G., 2021. Use of artificial neural networks for predicting volume of forest species in the Amazon Forest. Scientia Florestalis 49: e3610. https://doi.org/10.18671/scifor.v49n131.02.

Oliveira P.L.G., Matricardi E.A.T., Miguel E.P., Marimon Júnior B.H., Rezende A.V., 2024. Artificial Neural Network and Remote Sensing combined to predict the Aboveground Biomass in the Cerrado biome. Anais da Academia Brasileira de Ciências 96: e20221041. https://doi.org/10.1590/0001-3765202420221041.

Pennington R.T., Lehmann C.E.R., Rowland L.M., 2018. Tropical savannas and dry forests. Current Biology 28: R541-R545. https://doi.org/10.1016/j.cub.2018.03.014.

R Core Team, 2017. R: A language and environment for statistical computing. R Foundation for Statistical Computing, Vienna, Austria. [online 17 November 2019] URL: https://www.r-project.org/.

Ratter J.A., Bridgewater S., Ribeiro J.F., 2003. Analysis of the floristic composition of the Brazilian Cerrado vegetation - III: Comparison of the woody vegetation of 376 areas. Edinburgh Journal of Botany 60: 57-109. https://doi.org/10.1017/S0960428603000064.

Reis L.P., Souza A.L. de, Reis P.C.M. dos R., Mazzei L., Leite H.G., Soares C.P.B., Torres C.M.M.E., Silva L.F. da, Ruschel A.R., Rêgo L.J.S., 2019. Modeling of tree recruitment by artificial neural networks after wood harvesting in a forest in eastern Amazon rain forest. Ciência Florestal 29: 583–594. https://doi.org/10.5902/1980509825808.

Reis A.A. dos, Diniz J.M.F. de S., Acerbi Júnior F.W., Mello J.M. de, Batista A.P.B., Ferraz Filho A.C., 2020. Modeling the spatial distribution of wood volume in a Cerrado stricto sensu remnant in Minas Gerais state, Brazil. Scientia Forestalis 48: e2844. https://doi.org/10.18671/scifor.v48n125.15.

Rezende A.V., Vale A.T. do, Sanquetta C.R., Figuereido Filho A., Felfili J.M., 2006. Comparação de modelos matemáticos para estimativa do volume, biomassa e estoque de carbono da vegetação lenhosa de um cerrado sensu stricto em Brasília, DF. Scientia Forestalis 65–76.

Ribeiro J.F., Walter B.M.T., 2008. As principais fitofisionomias do bioma Cerrado. Sano S.M., Almeida S.P. de, Ribeiro J.F., (eds.), Cerrado: Ecologia e flora, Embrapa Cerrado, Planaltina, pp. 152-212.

Silva Júnior E.M. da, Maia R.D., Cabacinha C.D., 2018. Bee-inspired RBF network for volume estimation of individual trees. Computers and Electronics in Agriculture 152: 401–408. https://doi.org/10.1016/j.compag.2018.07.036.

Silva-Júnior C.M., 2012. 100 árvores do Cerrado Sentido Restrito. Rede de Sementes do Cerrado, Brasília, 360 p.

Silveira E.M.O., Reis A.A. dos, Terra M.C.N.S., Withey K.D., Mello J.M. de, Acerbi Júnior F.W., Ferraz Filho A.C., Mello C.R., 2019. Spatial distribution of wood volume in Brazilian savannas. Anais da Academia Brasileira de Ciências 91: e20180666. https://doi.org/10.1590/0001-3765201920180666.

Silveira E.M.O., Radeloff V.C., Martinuzzi S., Pastur G.J.M., Bono J., Politi N., Lizarraga L., Rivera L.O., Ciuffolu L., Rosas Y.M., Olah A.M., Gavier-Pizarro G.I., Pigeon A.M., 2023. Remote Sensing of Environment 285: 113391. https://doi.org/10.1016/j.rse.2022.113391.

Soper D.S., 2023. Using an Opportunity Matrix to Select Centers for RBF Neural Networks. Algorithms 16: 455. https://doi.org/10.3390/a16100455.

Sousa Júnior E., Freitas A., Rabelo R., Santos W., 2022. Estimation of Radial Basis Function Network Centers via Information Forces. Entropy 24: 1347. https://doi.org/10.3390/e24101347.

Sousa P.H.C. de, Sousa H.J. de, Chagas M.P., Binoti, D.H. B., Venturoli F., Resende R.T., 2023. Combining Digital Imaging and Artificial Neural Networks for Individual Volumetric Estimation of Non-Straight Trees. TreeDimensional Journal 11: e2023037, 1-10. https://doi.org/10.55746/treed.2023.12.037.

Souza Y.F. de, Miguel E.P., Lima A.J.N., Souza A.N., Matricardi E.A.T., Rezende A.V., Freitas J.V. de, Souza H.J. de, Oliveira K.N., Lima M.de F.B., Biali L.J., 2024. Generic and Specific Models for Volume Estimation in Forest and Savanna Phytophysiognomies in Brazilian Cerrado. Plants 13: 2769. https://doi.org/10.3390/plants13192769.

Thomas C., Andrade C.M., Schneider P.R., Finger C.A.G., 2006. Comparação de equações volumétricas ajustadas com dados de cubagem e análise de tronco. Ciência Florestal 16: 319–327. https://doi.org/10.5902/198050981911.

Xavier A.C.F., Silva-Neto C. de M., Martins T.O., Ferreira F.G., Monteiro M.M., Oliveira G.M. de, Venturoli F., 2017. Growth and volume of *Myracroduon urundeuva* Allemão after the year of silvicultural interventions. Australian Journal of Crop Science 11: 271-276. https://doi.org/10.21475/ajcs.17.11.03.pne360.

Yang W-C., Choe C-M., Kim J-S., Om M-S., Kim U-H., 2022. Materials selection method using improved TOPSIS without rank reversal based on linear max-min normalization with absolute maximum and minimum values. Materials Research Express 9: 065503. https://doi.org/10.1088/2053-1591/ac2d6b.

Zhang T., Cao Y., Ye F., Ren J., 2018. Use Multilayer Perceptron in Calibrating Multistage Non-linearity of Split Pipelined-ADC. IEEE International Symposium on Circuits and Systems (ISCAS), Florence, 5 p.

Zimbres B., Rodrígues-Veiga P., Shimbo J.Z., Bispo P. da C., Balzter H., Bustamante M., ..., Alencar A., 2021. Mapping the stock and spatial distribution of aboveground woody biomass in the native vegetation of the Brazilian Cerrado biome. Forest Ecology and Management 499: 119615. https://doi.org/10.1016/j.foreco.2021.119615.